

Electronic Supplementary Material (ESI) for Dalton Transactions.

This journal is © The Royal Society of Chemistry 2019

SUPPLEMENTARY MATERIAL

Syntheses and proton conduction properties of cucurbit[6]uril-based metal-organic rotaxane networks assembly by anion regulation strategy

Xue-Song Wu,^a Dong-Ming Cheng,^b Xin-Long Wang,^{a,b} Jing Sun,^{*a} Hong-Ying Zang^b and Zhong-Min Su^{*a,b}

^a Jilin Provincial Science and Technology Innovation Center of Optical Materials and Chemistry, School of Chemistry and Environmental Engineering, Changchun University of Science and Technology, Changchun, Jilin 130022, P. R. China.

^b National & Local United Engineer Laboratory for Power Batteries, Northeast Normal University, Changchun, Jilin 130024, P. R. China.

*Corresponding Author E-mail: sj-cust@126.com (J. Sun); zmsu@nenu.edu.cn (Z.-M. Su).

Experimental Section

Materials and physical Measurements.

[PR63]²⁺·2[NO₃]⁻ and CB[6] were synthesized according to references.^{1,2} The IR spectra were recorded using KBr pellets in the range of 4000–400 cm⁻¹ on a Mattson Alpha-Centauri spectrometer. Thermogravimetric analysis (TGA) was performed on a PerkinElmer TG-7 analyzer over the temperature 20–800 °C in a nitrogen-gas atmosphere with a heating rate of 10 °C min⁻¹. Powder X-ray diffraction (XRD) measurements were recorded on a Rigaku/Dmax 2200 pc diffractometer with Cu-Kα (λ = 1.5418 Å) radiation in the range 5–50°.

X-ray crystallographic study

The single-crystal X-ray diffraction measurements of all crystals were performed on a Bruker Apex II CCD equipped with graphite monochromated Mo-Kα radiation (λ = 0.71073 Å). The data of crystals were collected at room temperature. Multi-scan absorption corrections were applied using the SADABS program. The structure of crystals was solved by direct methods and refined by F2 full-matrix refinement using the SHELXTL package (SHELXTL-97). Carbon-bonded hydrogen atoms and nitrogen-bonded hydrogen atoms were placed in geometrically calculated positions; hydrogen atoms on water molecules were not assigned or directly included in the molecule formula. Further details of the X-ray structural analysis of compounds are given in Table S1 and bond lengths and angles are presented in Tables S2–S3.

Preparation of [Cu₃(PR63)(TA)₂Cl₂]·2H₂O (**1**).

A mixture of CuCl₂·2H₂O (45 mg, 0.26 mmol), [PR63]²⁺·2[NO₃]⁻ (80 mg, 0.06 mmol), racemic sodium tartrate (40 mg, 0.21 mmol), and 3.5 mL of H₂O was stirred for 5 min, and then transferred and sealed in a 18 mL Teflon-lined stainless steel container, which is heated at 120 °C for 48 h. Block green crystals of **1** suitable for X-ray crystallography were obtained, washed with distilled water, and dried in air. Yield: 40.6% based on [PR63]. Elemental analysis calc. for C₆₂H₇₂Cl₂Cu₃N₂₈O₂₆. (%): C 39.46, H 3.85, N 20.78; Found: C 38.94, H 3.59, N 21.03.

Preparation of [Cu₆(PR63)(TA)₄(H₂O)₄]·17H₂O (**2**).

2 was synthesized by a procedure similar to that was used for **1** with CuNO₃·3H₂O (45 mg, 0.19 mmol) instead of CuCl₂·2H₂O. Block blue crystals of **2** suitable for X-ray crystallography were

obtained, washed with distilled water, and dried in air. Yield: 44% based on [PR63]. Elemental analysis calc. for $C_{70}H_{110}Cu_7N_{28}O_{55}$. (%): C 31.50, H 4.15, N 14.70; Found: C 32.12, H 4.08, N 15.27.

Impedance analysis.

The samples were ground into homogeneous powder, and then the powder was compressed into pellets at 15 MPa for 1 min. The proton conduction behaviors of materials were measured on an IviumStat electrochemical workstation by alternating-current (AC) impedance measurements over the applied frequency range from 1 Hz to 1 MHz using a quasi-four-probe method with Pt-pressed electrodes under an applied voltage of 50 mV. The measurements were operated at temperatures (40 to 85 °C), with different relative humidities (75% to 97% RH). The proton conductivity was calculated using the following equation $\sigma = L/(RA)$ where σ = ion conductivity, L = thickness of the pellet, R = resistance of the pellet, and A = area of the pellet. The activation energy values were obtained from the slope of Arrhenius plots by least-squares fitting.

Table S1. Crystallographic Parameters and Structure Refinement Details for compounds **1** and **2**.

	Compound 1	Compound 2
formula	C ₆₂ H ₇₂ N ₂₈ O ₂₆ Cu ₃ Cl ₂	C ₇₀ H ₉₂ N ₂₈ O ₅₄ Cu ₇
formula mass	1887	2668.64
crystal system	Triclinic	Triclinic
space group	<i>P</i> ₁	<i>P</i> ₁
<i>a</i> /Å	11.980(5)	12.758(5)
<i>b</i> /Å	12.321(5)	14.636(5)
<i>c</i> /Å	12.797(5)	14.677(5)
<i>α</i> (°)	76.231(5)	80.719(5)
<i>β</i> (°)	75.919(5)	68.722(5)
<i>γ</i> (°)	83.363(5)	84.291(5)
V/Å ³	1776.2(12)	2517.8(16)
<i>Z</i>	1	1
<i>D</i> _c /g cm ⁻³	1.764	1.76
<i>μ</i> /mm ⁻¹	1.072	1.568
F(000)	969	1369
reflns collected	11403	36674
unique reflns	7138	8879
R _{int}	0.0243	0.0780
GOF	1.077	1.054
R ₁ ^a [<i>I</i> > 2σ(<i>I</i>)]	0.0482	0.0592
wR ₂ ^b (all data)	0.1671	0.1788

$$^a R_1 = \sum(|F_o| - |F_c|) / \sum F_o, \quad ^b wR_2 = [\sum w(|F_o|^2 - |F_c|^2)^2 / \sum w(F_o^2)]^{1/2}.$$

Table S2. Selected bond length (Å) for compound **1**.

Cu(1)-O(4)	1.925(3)	Cu(1)-N(1)	2.006(3)
Cu(1)-O(5)	1.942(3)	Cu(1)-Cl(1)	2.2909(14)
Cu(2)-O(2)	1.965(3)	Cu(2)-O(3)	2.420(3)
Cu(2)-O(4)	1.962(3)		

Table S3. Selected bond length (Å) for compound **2**.

Cu(1)-N(1)	1.999(5)	Cu(1)-O(1)	2.4530(5)
Cu(1)-O(2)	1.937(4)	Cu(1)-O(4)	1.953(4)
Cu(1)-O(13)	1.966(4)	Cu(1)-O(14)	2.7935(5)
Cu(2)-O(4)	1.927(4)	Cu(2)-O(5)	2.274(6)
Cu(2)-O(6)	1.975(4)	Cu(2)-O(12)	1.923(4)
Cu(2)-O(14)	1.965(4)	Cu(3)-O(5)	2.6505(75)
Cu(3)-O(6)	1.939(4)	Cu(3)-O(8)	1.912(4)
Cu(3)-O(9)	1.941(4)	Cu(3)-O(11)	1.921(4)
Cu(4)-O(11)	1.899(4)	Cu(4)-O(12)	1.930(4)

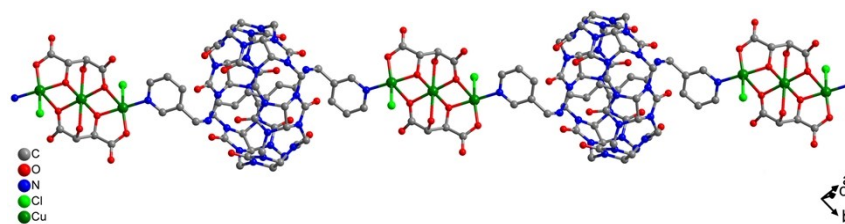


Fig. S1 The 1D straight chain in compound 1.

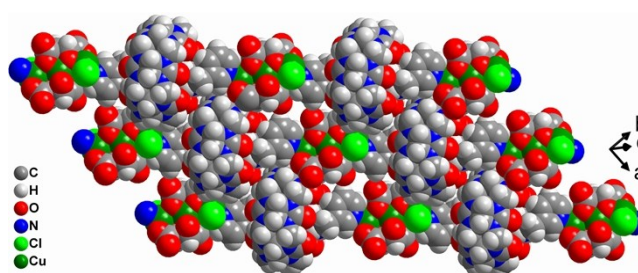


Fig. S2 The space-filling view of the 2D supramolecular networks in compound 1.

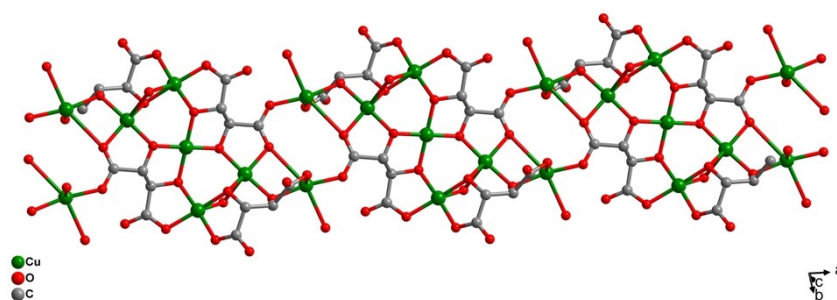


Fig. S3 The 1D copper carboxylic acid chain in compound 2.

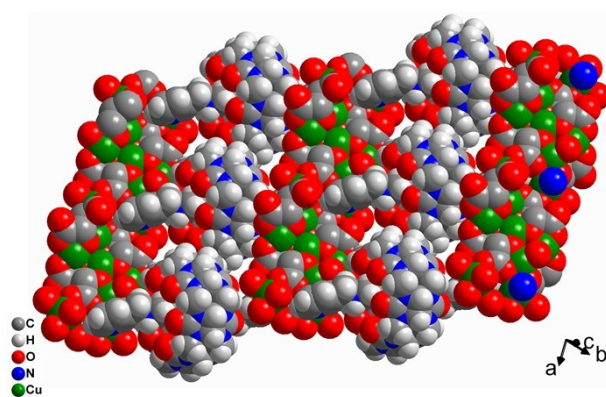


Fig. S4 The space-filling view of the 2D networks in compound 2.

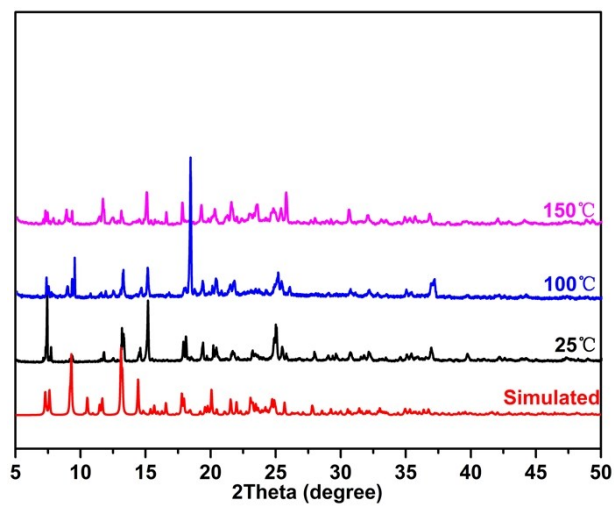


Fig. S5 Variable temperature PXRD patterns of 1.

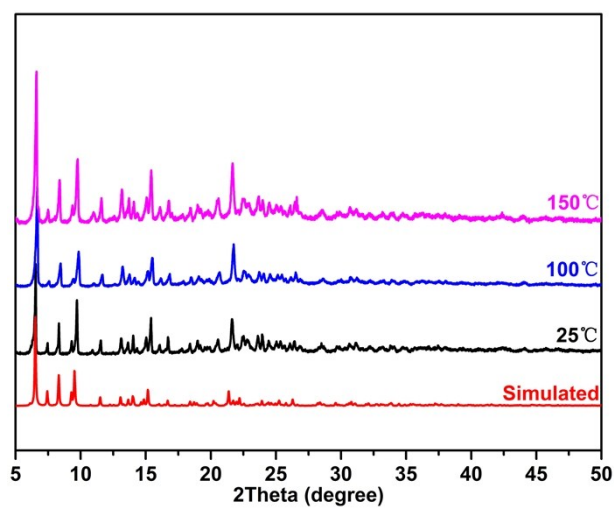


Fig. S6 Variable temperature PXRD patterns of 2.

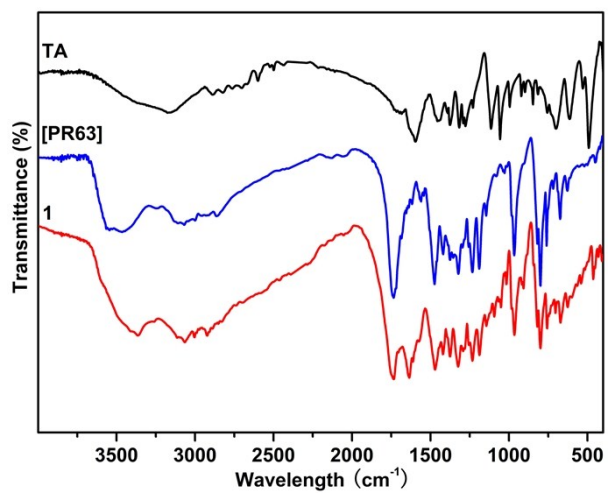


Fig. S7 Infrared absorption spectrum of TA, [PR63]²⁺·2[NO₃]⁻, compound 1.

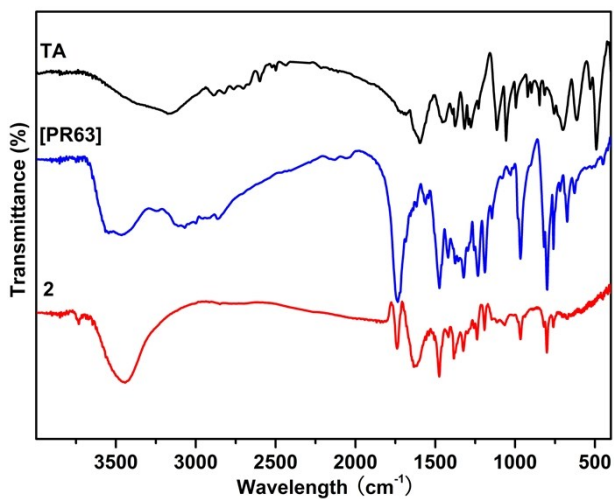


Fig. S8 Infrared absorption spectrum of TA, [PR63]²⁺·2[NO₃]⁻, compound 2.

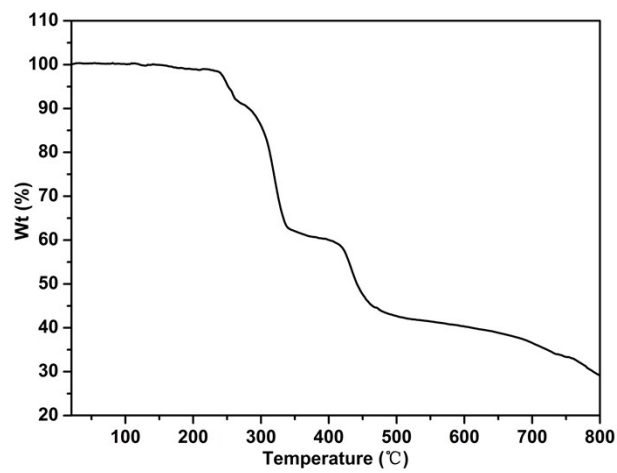


Fig. S9 TGA curve of compound 1.

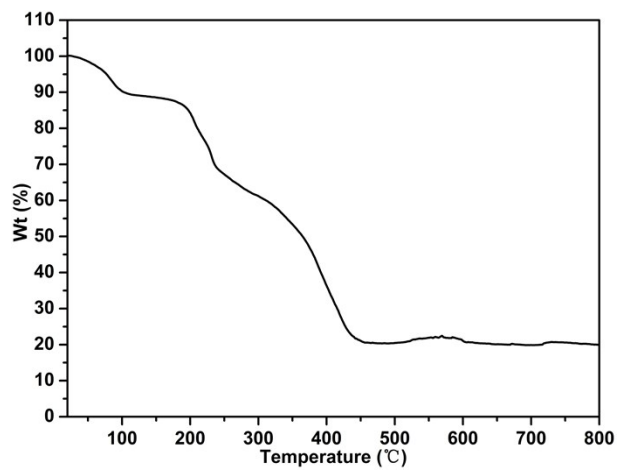


Fig. S10 TGA curve of compound 2.

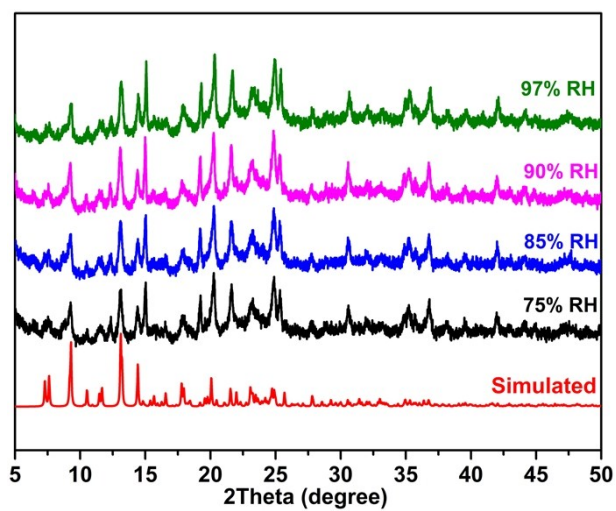


Fig. S11 PXR D patterns of compound 1 and compound 1 with different relative humidity.

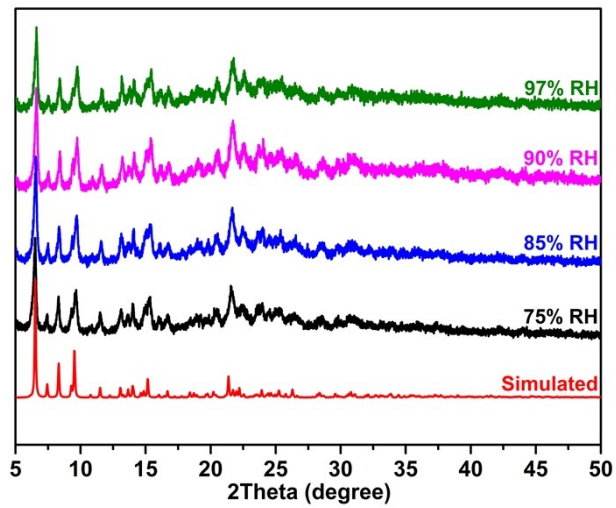


Fig. S12 PXR D patterns of compound 2 and compound 2 with different relative humidity.

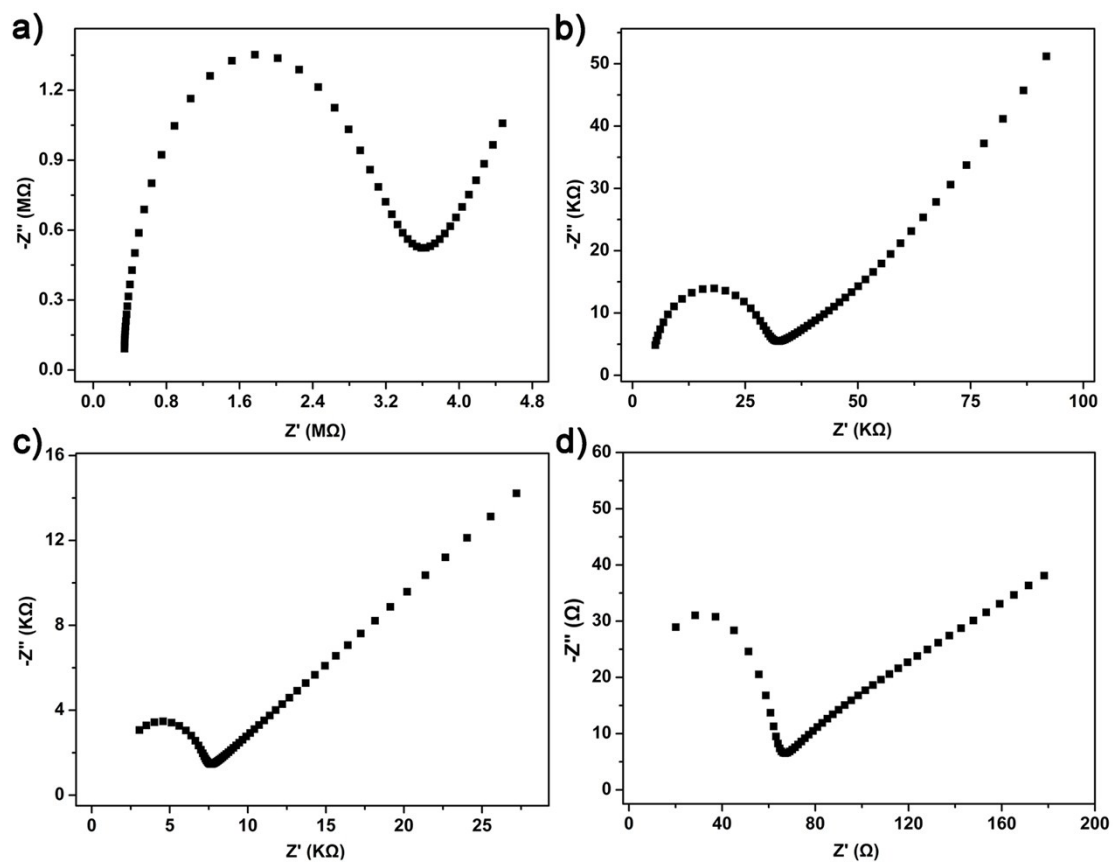


Fig. S15 Nyquist plot of 2 at 60 °C and 75% RH (a), 85% RH (b), 90% RH (c) and 97% RH (d).

Table S4. Comparison of proton conductivity of compound **1** and **2** in this work with some other representative MOF proton conductors.

Compounds	σ (S cm ⁻¹)	Ea (eV)	Reference
Compound 1	2.82×10^{-4} (85°C, 97% RH)	0.75	This work
Compound 2	2.85×10^{-3} (85°C, 97% RH)	0.30	This work
H₃L ·0.5[Cu ₂ (OH) ₄ ·6H ₂ O]·4H ₂ O	5.5×10^{-3} (60°C, 95% RH)	0.52	3
[Cu ^I ₃ Cu ^{II} ₃ L ₃ (DMF) ₂ (CH ₃ OH)(H ₂ O)]·3CH ₃ OH	3.78×10^{-4} (100°C, 98% RH)	0.61	4
{[Cu(H ₂ bpdc)(H ₂ O) ₂ Cl _{0.5}] ₂ [PW ₁₂ O ₄₀]}·10H ₂ O	1.40×10^{-3} (100°C, 98% RH)	0.52	5
{[Cu(H ₂ bpdc)(H ₂ O) _{2.5}] ₂ [SiW ₁₂ O ₄₀]}·10H ₂ O	1.77×10^{-3} (100°C, 98% RH)	0.57	5
[Cu ₄ Cu _{II} ₄ L ₄] _n -NH ₃	1.13×10^{-2} (100°C, 98% RH)	0.39	6
[Cu(p-IPhHIDC)] _n	1.51×10^{-3} (100°C, 98% RH)	1.79	7
Im@(NENU-3)	1.82×10^{-2} (70°C, 90% RH)	0.57	8
HKUST-1	1.08×10^{-8} (90°C, 70% RH)	0.69	9
NENU-3	4.76×10^{-5} (90°C, 70%RH)	0.41	9
NENU-3-Ina	1.81×10^{-3} (90°C, 70%RH)	0.36	9
Cu ₄ (L) ₂ (OH) ₂ (DMF) ₂	7.4×10^{-4} (95°C, 95% RH)	1.32	10
{[H ₃ O][Cu ₂ (DSOA)(OH)(H ₂ O)] _{9.5} H ₂ O} _n	1.9×10^{-3} (85°C, 98% RH)	1.04	11
{[Cu ₃ (L) ₂ (H ₂ O) ₄][Cu(dmf) ₄ (SiW ₁₂ O ₄₀)] ₉ H ₂ O} _n	5.94×10^{-4} (100°C, 98% RH)	0.32	12

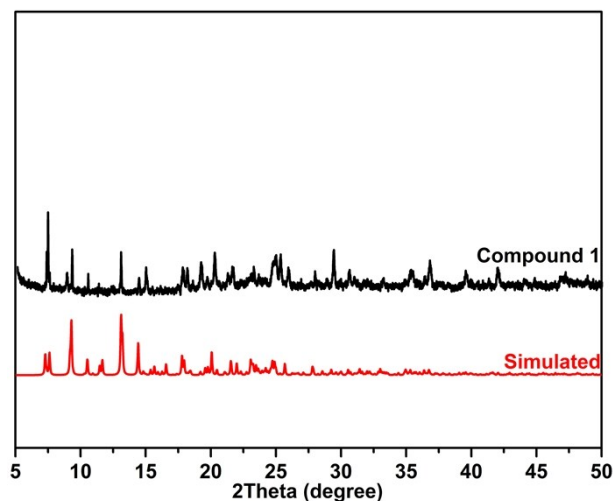


Fig. S16 PXRD patterns of **1** after impedance analysis.

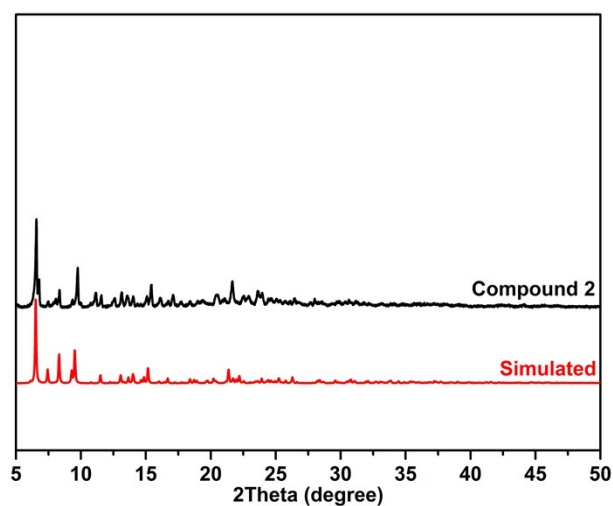


Fig. S17 PXRD patterns of **2** after impedance analysis.

References

- 1 Z.-B. Wang, H.-F. Zhu, M. Zhao, Y.-Z. Li, T.-a. Okamura, W.-Y. Sun, H.-L. Chen and N. Ueyama, *Cryst. Growth Des.*, 2006, **6**, 1420-1427.
- 2 D. Bardelang, K. A. Udachin, D. M. Leek, J. C. Margeson, G. Chan, C. I. Ratcliffe and J. A. Ripmeester, *Cryst. Growth Des.*, 2011, **11**, 5598-5614.
- 3 S. Nakatsuka, Y. Watanabe, Y. Kamakura, S. Horike, D. Tanaka and T. Hatakeyama, *Angew. Chem., Int. Ed.*, DOI:10.1002/anie.201912195.
- 4 Z.-B. Sun, Y.-L. Li, Z.-H. Zhang, Z.-F. Li, B. Xiao and G. Li, *New J. Chem.*, 2019, **43**, 10637-10644.
- 5 H. Yang, X.-Y. Duan, J.-J. Lai and M.-L. Wei, *Inorg. Chem.*, 2019, **58**, 1020-1029.
- 6 R. Liu, L. Zhao, S. Yu, X. Liang, Z. Li and G. Li, *Inorg. Chem.*, 2018, **57**, 11560-11568.

- 7 Z. Sun, S. Yu, L. Zhao, J. Wang, Z. Li and G. Li, *Chem. Eur. J.*, 2018, **24**, 10829-10839.
- 8 Y. Ye, W. Guo, L. Wang, Z. Li, Z. Song, J. Chen, Z. Zhang, S. Xiang and B. Chen, *J. Am. Chem. Soc.*, 2017, **139**, 15604-15607.
- 9 Y. Liu, X. Yang, J. Miao, Q. Tang, S. Liu, Z. Shi and S. Liu, *Chem. Commun.*, 2014, **50**, 10023-10026.
- 10 X. Meng, S.-Y. Song, X.-Z. Song, M. Zhu, S.-N. Zhao, L.-L. Wu and H.-J. Zhang, *Chem. Commun.*, 2015, **51**, 8150-8152.
- 11 X.-Y. Dong, R. Wang, J.-B. Li, S.-Q. Zang, H.-W. Hou and T. C. W. Mak, *Chem. Commun.*, 2013, **49**, 10590-10592.
- 12 M.-L. Wei, J.-J. Sun, X.-Y. Duan, *Eur. J. Inorg. Chem.*, 2014, **2014**, 345-351.